Sustainability, Agri, Food and Environmental Research, (ISSN: 0719-3726), 12(X), 2024:
http://dx.doi.org/

Finite element analysis of laminated composite stiffened hyperbolic paraboloid hyparshell subjected to impact loading.

Análisis de elementos finitos de un hyparshell paraboloide hiperbólico rígido compuesto laminado sometido a carga de impacto.

Irshad, A[1], Neogi, S.D[1]

[1] Department of Civil Engineering, Techno International New Town, Kolkata, West Bengal, India

Corresponding author's email: asheequlirshad@gmail.com (Irshad A.)

ABSTRACT

Laminated composite has produced a solution in the weight-sensitive branches of Engineering due to its low specific weight, high specific strength, and weathering resistance. It is its low transverse shear capacity under impact load has become a great concern for researchers for its successful implementation in different industrial sectors. The impact which is likely to occur in cyclone-prone zones and aircraft bases where wind-borne debris causes the same. The sudden strike may cause delamination, crack in the epoxy medium or tearing of fibers which remain suppressed under the lamina and eventually causes collapse. This study is an effort to analyze the laminated composite hyparshell under impact load with simply-supported boundary conditions. Installation of stiffeners in various positions becomes unavoidable in certain cases and which is optimized and the best possible combination is concluded. A detailed comparative study of deformation, stress and strain is done with respect to various impactor velocities.

Keywords: laminated composite stiffened hyparshell; impact

RESUMEN

El compuesto laminado ha producido una solución en las ramas de la ingeniería sensibles al peso debido a su bajo peso específico, alta resistencia específica y resistencia a la intemperie. Es su baja capacidad de corte transversal bajo carga de impacto lo que se ha convertido en una gran preocupación para los investigadores para su implementación exitosa en diferentes sectores industriales. El impacto, que probablemente se producirá en zonas propensas a ciclones y en bases de aeronaves donde los desechos transportados por el viento, causan lo mismo. El golpe repentino puede provocar delaminación, grietas en el medio epoxi o desgarro de las fibras que permanecen reprimidas debajo de la lámina y eventualmente provocan el colapso. Este estudio es un esfuerzo por analizar el hyparshell compuesto laminado bajo carga de impacto con condiciones de contorno simplemente apoyadas. En determinados casos es inevitable la instalación de refuerzos en diferentes posiciones, lo que se optimiza y consigue

la mejor combinación posible. Se realiza un estudio comparativo detallado de la deformación, la tensión y la deformación con respecto a diversas velocidades del impactador.

Palabras clave: hyparshell rígido de composite laminado; impacto

INTRODUCTION

Laminated composites have been discovered and adopted as a result of the hunt towards smarter materials. Given this material's excellent stiffness to weight ratio, it has become extremely popular. Due to the existence of two or more materials in a single domain, mathematical modeling of composite materials is a complex process in and of itself. Despite having a wide range of benefits, laminated composites are more susceptible to damage from impacts than traditional building materials like steel and concrete because they are weak in transverse shear. It goes without saying that one of the most critical parts in the analysis of an impact response problem is the precise modelling of contact behavior. Several studies have frequently used the Hertz-derived classical contact law for elastic solids. In the case of composite materials, the issue becomes more complicated, and the Hertzian contact law—which was derived for homogeneous isotropic materials—might not be appropriate. To establish an empirical indentation law considering indentation consideration, Tan and Sun [2] carried out an experimental programme on a graphite/epoxy laminated plate. Nine-nodded plate finite element was used to verify the theory supporting their experiment. Chen and Sun [3] reported the time histories of the contact force and displacement for the simply supported plate and the initially stressed plate during impact. The Tan and Sun [2] proposed contact law was applied. They used a composite plate having ten layers that were supported simply as the impacted mass, and a steel ball as the impactor. Their analysis cleared out any issues with shell shapes. Toh et al initial's paper on impact analysis of shell structure [4] for an orthotropic laminated cylindrical shell under low-velocity impact caused by a solid striker. Glass/epoxy laminated composite ogival shells subjected to a low-velocity impact at any arbitrary position by a solid striker were investigated by Shim et al. [5] for their elastic response. An analytical biharmonic polynomial solution was reported. Kistler and Waas [6] proposed a finite element model with and without geometric nonlinearity for a laminated composite cylindrical shell subjected to transverse center impact. By using the finite-element approach and Fourier series, Krishnamurthy et al. [7] investigated the impact response and subsequent damage of a laminated composite shell struck by a metallic impactor for a cylindrically curved panel. Karmakar et al. [8,9] conducted a transient dynamic finite element analysis to investigate the behavior of rotating and centrally impacted delaminated composite pre-twisted cylindrical shells. Their research examined the effects of rotational inertia and transverse shear deformation [9]. Yiming et al. [10] studied the damage analysis and dynamic response of an orthotropic shallow spherical shell made of an elastoplastic laminated composite under low-velocity impact. The impact response of shell structures used in civil engineering has not received enough attention, even though these shells may frequently be subjected to impact loads, according to a review of the literature. Snowfall, airborne debris in cyclone-prone zones, and other circumstances all result in impact forces on shell roofs. Therefore, it is felt that shell roof impact response has to be studied. Although Sahoo and Chakravorty [11],[12],[13] have reported on several

significant characteristics of these shell morphologies, a comparable review in the field of composite shells shows that the industrially significant hypar shell needs much more attention. Das Neogi reported the impact response behavior of simply supported skewed hyparshell roofs by the finite element method [15].

Commonly referred to as hyper shells, hyparbolic paraboloid shells with straight edges are aesthetically pleasing doubly curved anticlastic surfaces that are simple to construct because they are doubly ruled. They are preferred as roofing units in many practical situations that call for large column-free spaces. It is most commonly seen in stadiums and airports. Moreover, stiffeners are required to control the excessive deformation brought on by these impacts. Therefore, this study aims to conduct a numerical investigation of laminated composite stiffened hyparbolic paraboloid hyparshell subjected to impact. The surface of the hyparbolic paraboloid hyparshell is shown in Fig. 1.

MATHEMATICAL FORMULATION

The basic mass and stiffness matrices of the skewed hypar shell adopted in the present paper follow the equations and relations as reported by Sahoo and Chakravorty [11,13]. Fig. 2 and 3 illustrate the FE model of hyparshell and the schematic diagram of impact formulation respectively.

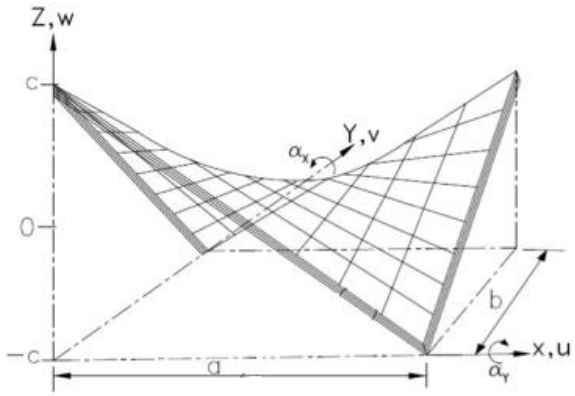

Fig. 1. Surface of a hyparbolic paraboloid hyparshell

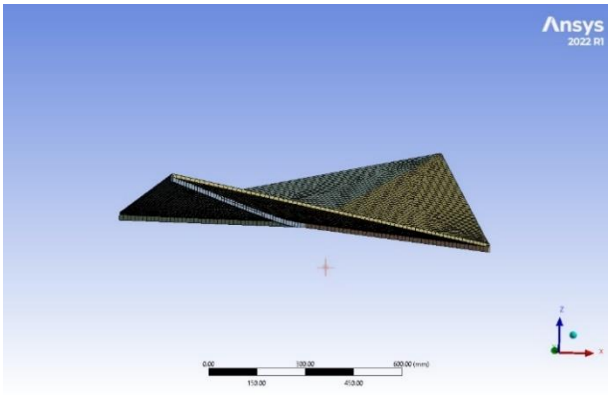

Fig. 2. FE model of hyparshell in Ansys

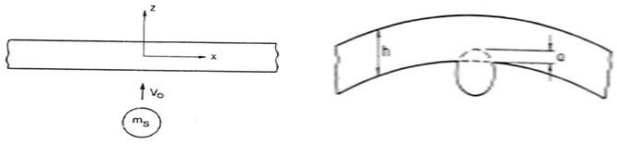

Fig. 3. Schematic diagram of impact formulation

The dynamic equilibrium equation of the target shell for low-velocity impact is given by the following equation:

$$[M]\{\ddot{\delta}\}+k\{\delta\}=\{F\} \quad (1)$$

where [M] and [K] are global mass and elastic stiffness matrices, respectively. {δ} is the global displacement vector. For the impact problem, {F} is given as

{F}={0 0 0 ….F_C……0 0 0}T

(2)

Here F_C is the impact force given by the indentation law and the equation of motion of the rigid impactor is given as

$$m_i \ddot{\omega}_i + F_C = 0 \quad (3)$$

where mi and $\ddot{\omega}_i$ are the mass and acceleration of the impactor respectively. The evaluation of the contact force depends on a contact law that relates the contact force with indentation. The contact force model following Chen and Sun [3] has been incorporated into the present finite element formulation. If k is the contact stiffness and αm is the maximum local indentation, the contact force Fc during loading is evaluated as [3]

$$F_c = k\alpha^{1.5} \qquad 0<\alpha\leq\alpha_m \quad (4)$$

The solution for the equations of motion given by Equations (1) and (3) is solved using the Newmark constant-acceleration time integration algorithm in the present analysis. Equation (1) may be expressed in the iteration form at each time step.

$$\left[\bar{K}\right]\{\Delta\}_{t+\Delta t}^{i+1} = \frac{\Delta t^2}{4}\{F\}_{t+\Delta t}^{i} + [M]\{b\}_i \quad (5)$$

Where,

$$\left[\bar{K}\right] = \frac{\Delta t^2}{4}[K] + [M] \quad (6)$$

$$\{b\}_t = \{\Delta\}_t + \Delta t\left\{\dot{\Delta}\right\}_t + \frac{\Delta t^2}{4}\left\{\ddot{\Delta}\right\}_t \quad (7)$$

The same solution scheme is also utilized for solving the equation of motion of the impactor. It is to be noted that a modified contact force obtained from the previous iteration is used to solve the current response. The iteration procedure is continued until the equilibrium criterion is met.

NUMERICAL EXAMPLE

Problems are solved with two different objectives. The present formulation is applied to solve natural frequencies of graphite-epoxy twisted plates which are structurally similar to skewed hyparshells. This problem is expected to validate both the stiffness and mass matrix formulation of the present finite element code. Another problem, solved earlier by Sun and Chen [3] regarding the impact response of composite plate, is taken up as the second benchmark to validate the impact formulation. The details of the benchmark problems are furnished along with Table 1 and Fig. 4.

Table 1. Nondimensional natural frequencies for three-layer graphite epoxy twisted plates

Angle of twist	Θ deg.	0°	15°	30°	45°	60°	75°	90°
Θ = 15°	Qatu and Lessia [14]	1.00	0.93	0.74	0.53	0.35	0.27	0.26
	Present Formulation	0.98	0.92	0.77	0.51	0.33	0.28	0.26
Θ = 30°	Qatu and Lessia [14]	0.96	0.89	0.72	0.52	0.34	0.26	0.24
	Present Formulation	0.95	0.87	0.71	0.53	0.33	0.25	0.23

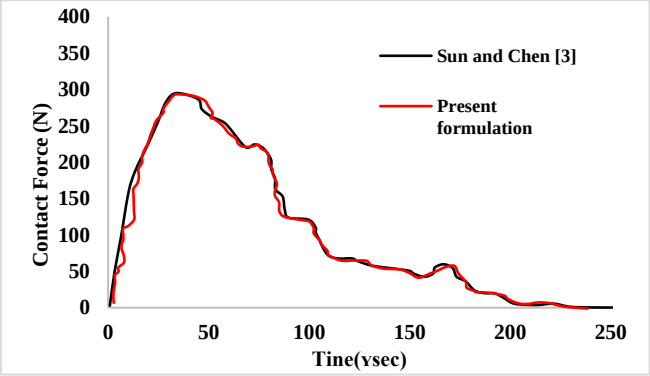

Fig. 4. Contact force history of simply supported plate

Apart from the problems mentioned above, the impact response of hyparbolic paraboloid hyparshells being impacted at the central point is also studied for simply supported boundary conditions and impact velocities. The details of the problems which are the authors' own are given below.

Boundary condition: - Simply supported (SS)

Lamination: - 0° / 90° (CP)

The velocity of impact (m/s): - 1 3, 5, 10

Details of shell geometry: - 1.0m, b =1.0m, t=0.01m, c=0.2m, c' = 0.1m

Material details: - E_{11}=120GPa, E_{22}=7.9 GPa, G_{12}=G_{23}=G_{13}= 5.5GPa

The indenter is struck centrally on the hypar shell from a finite distance which is constant for all the models. The mesh size is to be optimized at 4mm, considered for all models. 4 noded linear explicit elements are used in modeling the above-mentioned numerical problem.

The following cases are considered concerning the position of the stiffeners as shown in Fig. 5:

Case I: Hyparshell without stiffeners

Case II: Hyparshell with X-stiffener (along the parabola)

Case III: Hyparshell with Y-stiffener (along the straight edge)

Case IV: Hyparshell with X and Y stiffeners

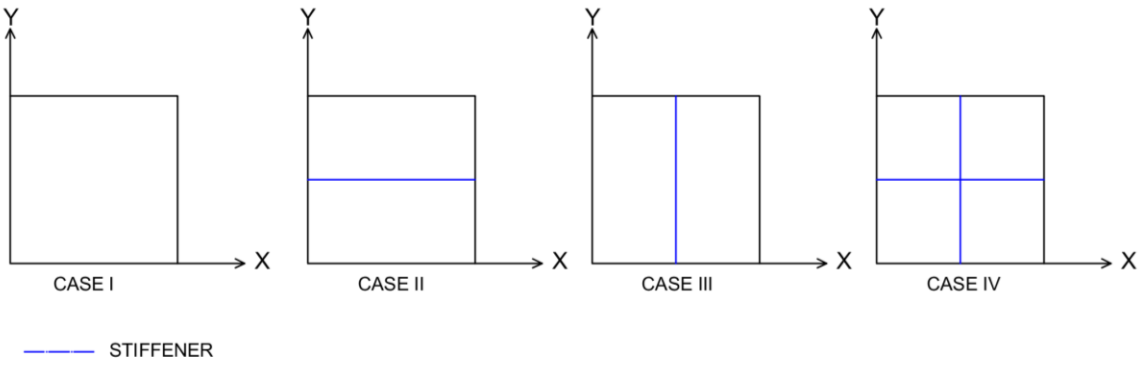

Fig. 5. Position of stiffeners

RESULTS AND DISCUSSION

The results in Table 1 show that the fundamental frequency values of the twisted plates obtained by the present formulation agree very closely with those reported by Qatu and Lessia [14]. This agreement validates the correct incorporation of stiffness and mass matrix formulation in the present code. Fig. 4 shows the time variation of the contact force induced in a composite plate under low-velocity impact previously reported by Sun and Chen [3]. The values obtained by the present formulation are also presented graphically in the same figure in a different style. Here again, excellent agreement of results is observed which establishes the correctness of impact formulation.

To study the impact response of simply supported (SS) cross-ply (CP) shell Fig. 6. to 29 and Table-II are studied. All the results of contact force, maximum deformation, maximum principal stress, maximum principal strain, Equivalent static load (ESL), and Dynamic magnification factor (DMF) obtained are presented in either graphical or tabular form and are arrived at after the study of time step convergence. The finite element mesh adopted is also based on force and displacement convergence criteria.

The impact force history of different velocities reveals that there is a spike in the contact force when the

impactor strikes the shell, almost like an impulse and it decays down to a null value as the impactor bounces back and loses connection with the shell. It is observed that the higher the velocity of the impactor higher is the impact force.

The maximum deformation is reduced considerably by the presence of the stiffeners. The combination of X and Y stiffeners provides the best results followed by the X and Y stiffeners individually. Maximum principal strain and stresses are also directly proportional to the impactor velocity. For both the mentioned parameters, Case IV provides the most favorable results.

To estimate the equivalent static load (ESL) corresponding to a particular impactor velocity, a concentrated load at the center (point of impact) is applied and adjusted the yield a central displacement equal to the maximum dynamic displacement. It is further explored to estimate the magnitude of the central displacement when the peak contact force is applied at the point of impact as a static concentrated load. The central displacement obtained under such a load when divides by the maximum dynamic displacements yields a dynamic magnification factor (DMF). The variations of maximum contact force, maximum dynamic displacement, and equivalent static load (ESL) with impactor velocity are almost linear, and of three above-mentioned values are increasing functions of impactor velocity. However, the dynamic magnification factor (DMF) and the impactor velocity show a logarithmic relation and the DMF is a decreasing function of velocity.

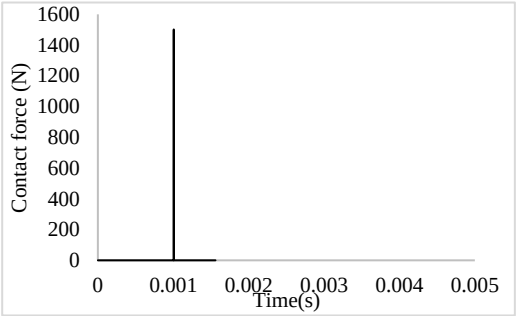

Fig. 6. Contact Force v/s Time for 1m/s (Case I)

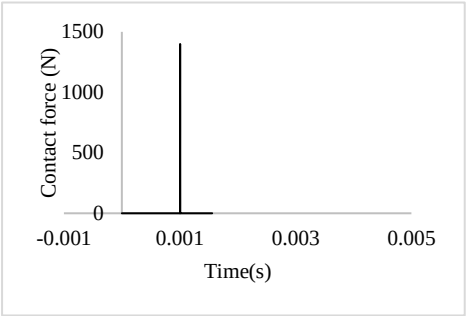

Fig. 7. Contact Force v/s Time for 1m/s (Case II)

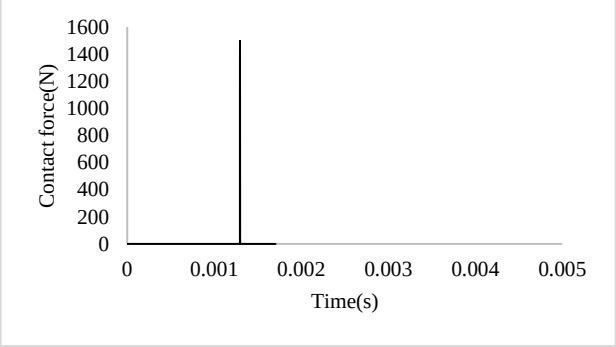

Fig. 8. Contact Force v/s Time for 1m/s (Case III)

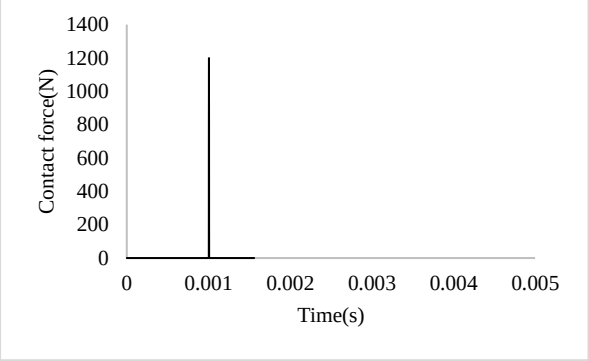

Fig. 9. Contact Force v/s Time for 1m/s (Case IV)

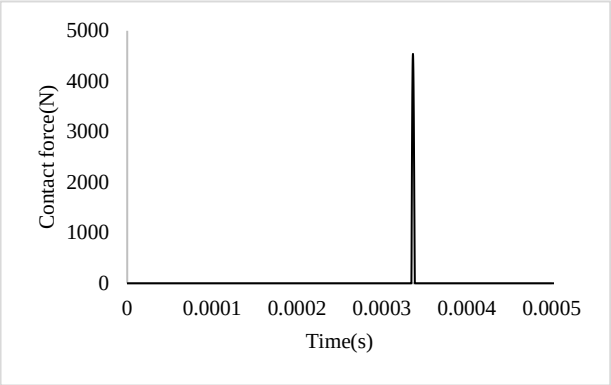

Fig. 10. Contact Force v/s Time for 3m/s (Case I)

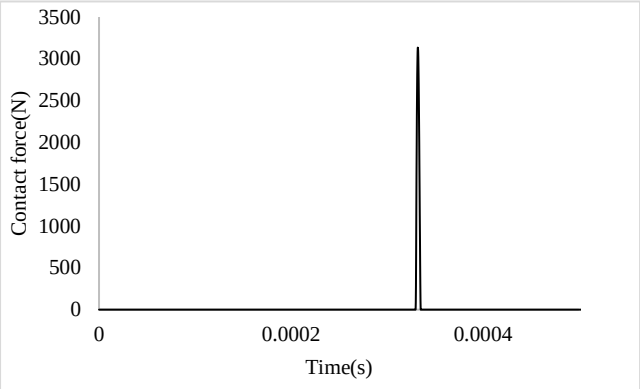

Fig. 11. Contact Force v/s Time for 3m/s (Case II)

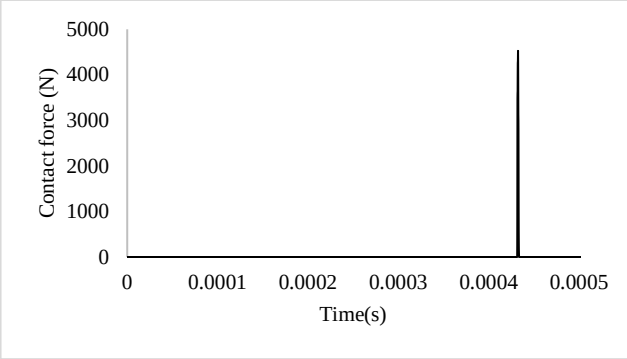

Fig. 12. Contact Force v/s Time for 3m/s (Case III)

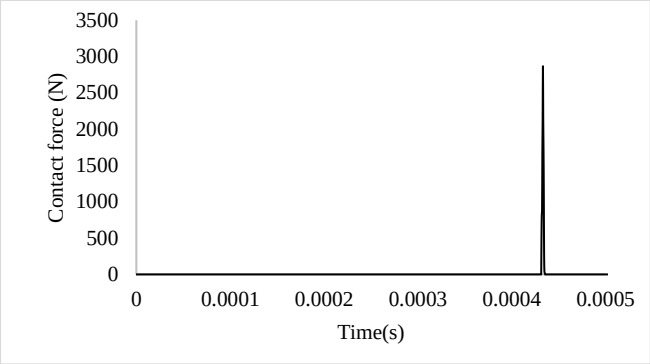

Fig. 13. Contact Force v/s Time for 3m/s (Case IV)

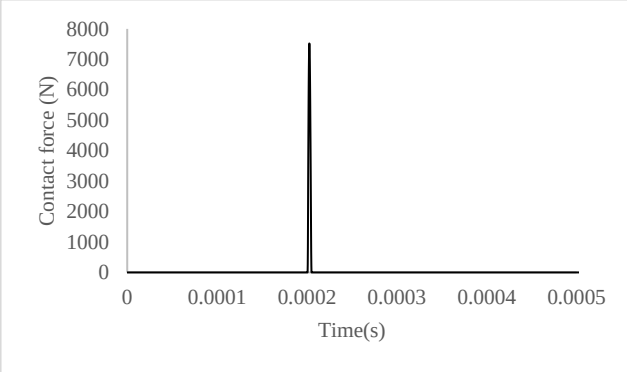

Fig. 14. Contact Force v/s Time for 5m/s (Case I)

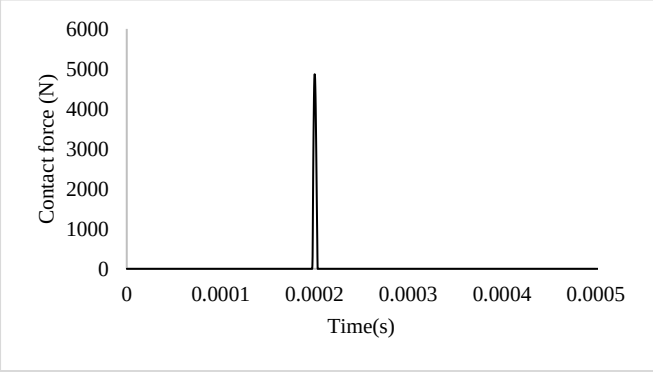

Fig. 15. Contact Force v/s Time for 5m/s (Case II)

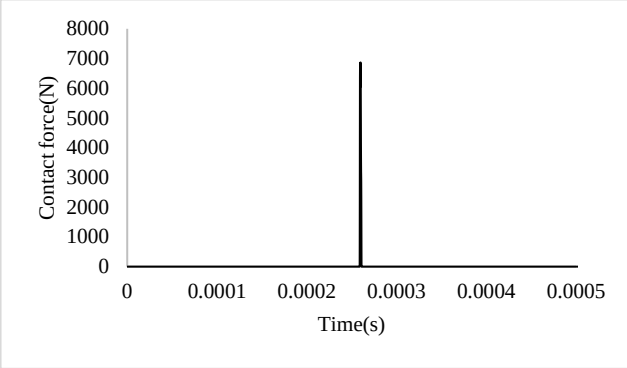

Fig. 16. Contact Force v/s Time for 5m/s (Case III)

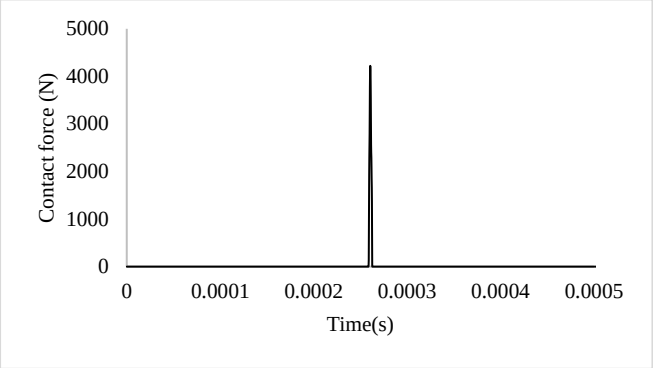

Fig. 17. Contact Force v/s Time for 5m/s (Case IV)

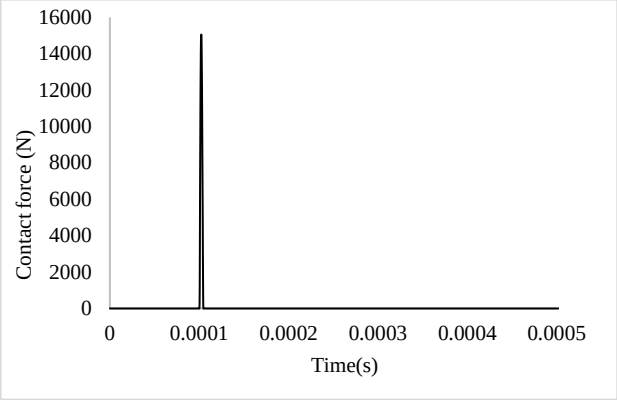

Fig. 18. Contact Force v/s Time for 10m/s (Case I)

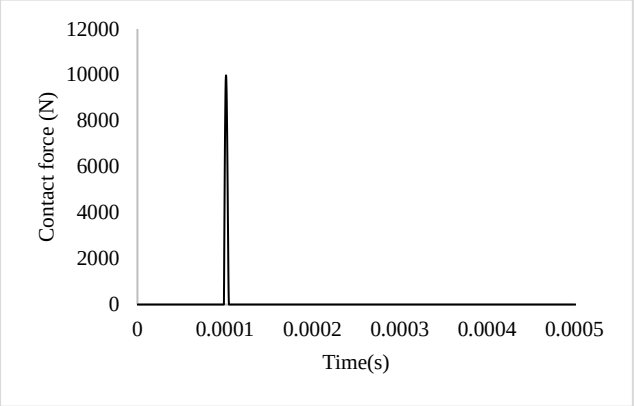

Fig. 19. Contact Force v/s Time for 10m/s (Case II)

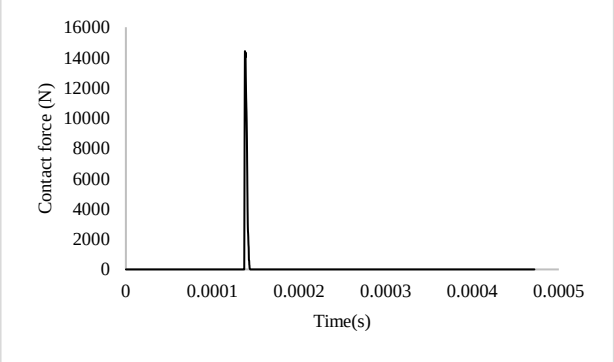

Fig. 20. Contact Force v/s Time for 10m/s (Case III)

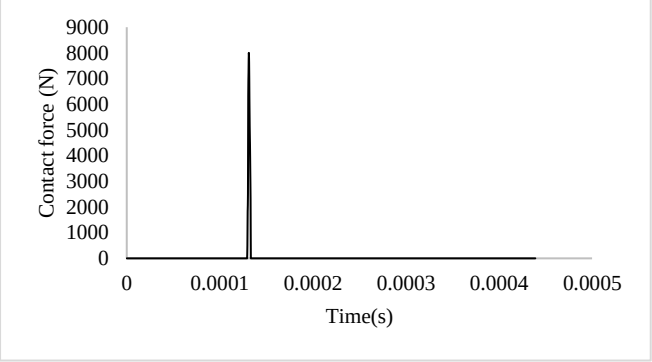

Fig. 21. Contact Force v/s Time for 10m/s (Case IV)

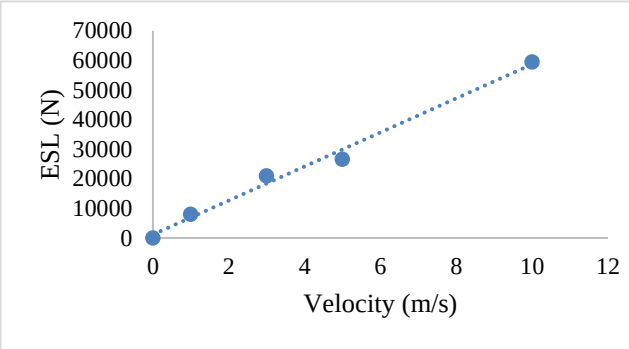

Fig. 22. ESL v/s Velocity (Case I)

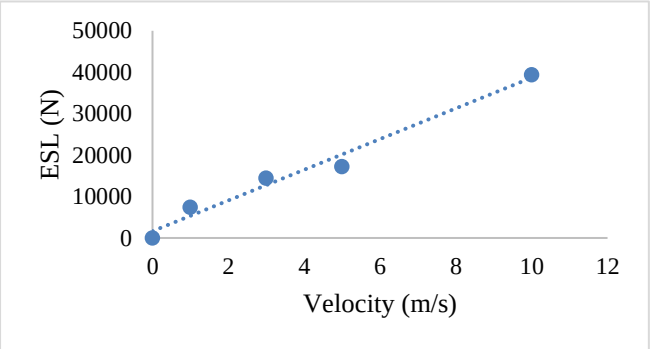

Fig. 23. ESL v/s Velocity (Case II)

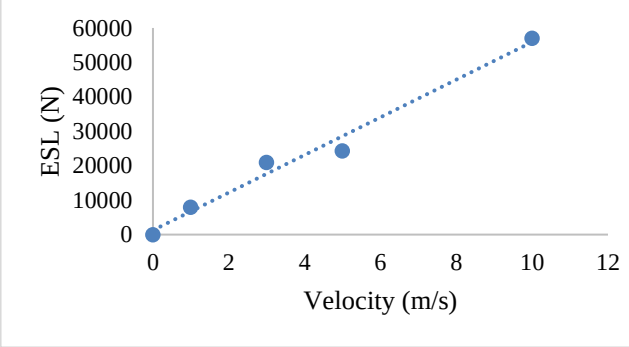

Fig. 24. ESL v/s Velocity (Case III)

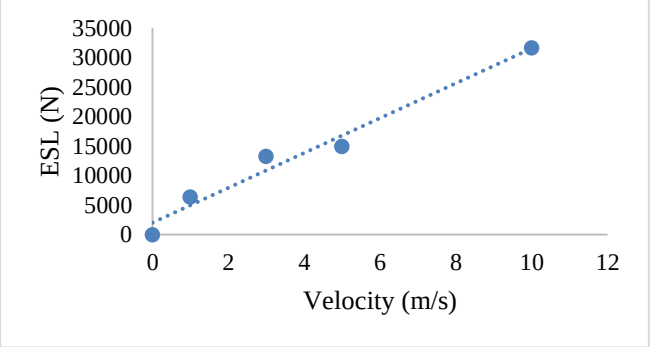

Fig. 25. ESL v/s Velocity (Case IV)

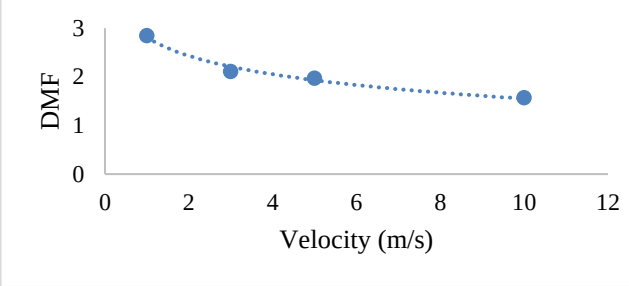

Fig. 26. DMF v/s Velocity (Case I)

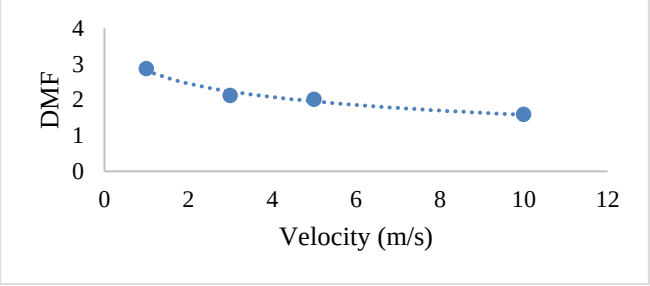

Fig. 27. DMF v/s Velocity (Case II)

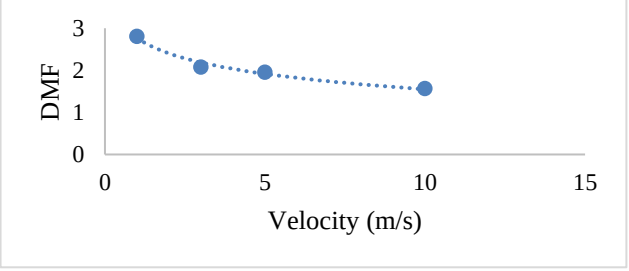

Fig. 28. DMF v/s Velocity (Case III)

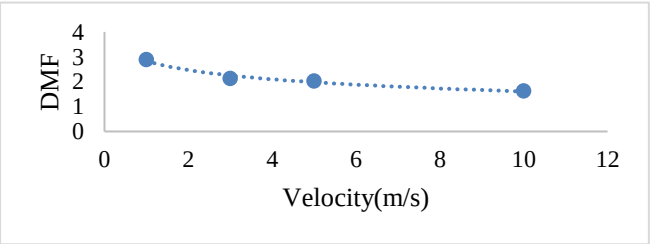

Fig. 29. DMF v/s Velocity (Case IV)

Table 2. Maximum Impact load, principal stress, principal strain, ESL & DMF of various velocities

Case No.	Impactor Velocity (m/s)	Maximum Impact load (N)	Maximum deformation (mm)	Maximum principal stress (MPa)	Maximum principal strain	ESL (N)	DMF
	0	0	0	0	0	0	0
	1	1501.7	1.5602	14.854	0.0012179	8004.06	1.57
I	3	4542.9	2.5163	42.502	0.0034624	20988.1	1.97
	5	7521.3	3.2763	67.478	0.0054241	26625.4	2.11
	10	15051	5.0664	127.8	0.010265	59451.4	2.85
	0	0	0	0	0	0	0
	1	1399.6	0.6994	13.017	0.0002225	7459.86	1.59
II	3	3134.4	2.3004	41.713	0.0009046	14480.9	2.01
	5	4862.8	2.9362	51.52	0.0020733	17214.3	2.12
	10	9981.4	4.9524	83.3885	0.0087216	39426.5	2.87
	0	0	0	0	0	0	0
	1	1496.3	0.7053	12.278	0.001013	7975.27	1.57
III	3	4527.2	2.4047	35.865	0.002876	20915.6	1.96
	5	6865	3.0302	57.204	0.004651	24302.1	2.08
	10	14421	4.7189	111.58	0.009502	56962.9	2.81
	0	0	0	0	0	0	0
	1	1199.6	0.63943	6.46	0.000166	6393.86	1.63
IV	3	2867.35	1.7636	21.545	0.000880	13247.1	2.03
	5	4221.1	2.8176	46.628	0.001295	14942.6	2.13
	10	8000.47	4.3913	64.88	0.008352	31601.8	2.89

CONCLUSIONS

The following conclusions may be derived from the present study.

1. The close agreement of the results obtained by the present method with those available in the published literature establishes the correctness of the approach used here.

2. Under the influence of normal low-velocity impact, the contact force shows a parabolic combined loading and unloading curve with a single peak for the practical class of shells considered here. Higher magnitude of impact velocity results in a higher value of the peak contact force. However, due to a sharp elastic rebound, the total duration of contact force is less for the higher velocity of the impactor.

3. The time instants at which the maximum contact force and the maximum dynamic displacement occur show a phase difference and interestingly in some cases the maximum displacement and hence stresses may occur even after the contact force dies down totally. Thus, it is concluded that the study should be continued only after when the major peaks of the dynamic displacement die down and not after the full decay of the contact force only.

4. The maximum contact force, the peak dynamic displacement, and the equivalent static load are all increasing functions of impactor velocity, the relations being almost linear. However, the dynamic magnification factor shows a logarithmically decreasing tendency with an increase of the velocity of impact.

5. Thorough numerical investigation of all the mentioned cases reveals that the combination of X and Y stiffeners is most favorable for considerable reduction of deformation and generation of stresses.

NOMENCLATURE

a, b	length and width of the shell
c	rise of hypar shell.
$\{d\}$	global displacement vector.
$\{d_e\}$	element displacement vector.
D	flexural rigidity of the shell
E_{11}, E_{22}	elastic moduli
G_{12}, G_{13}, G_{23}	shear moduli of a lamina
ρ	density
h	shell thickness

REFERENCES

Hertz H. (1881) On the contact of elastic solids, Journal fur die reine und angewandte Mathematik, 92,156-171

Tan, T.M. Sun, C.T., (1983) Use of statical indentation laws in the impact analysis of laminated composite plate. Journal of Applied Mechanics.52,6-12

Sun C.T., Chen, J.K., (1985) On the impact of initially stressed laminates, Journal of Composite Material. 19, 490-503

Toh S.L., Gong S.W., Shim V.P.W. (1995) Transient stress generated by low-velocity impact on the orthotropic laminated cylindrical shell, Composite Structures,31(3),213-228

Shim V.P.W., Toh S.L., Gong S.W., (1996) The elastic impact response of glass/epoxy laminated ogival shells, International Journal of Impact Engineering, 18(6) 633-655

Kistler L.S., and Waas, A.M., (1998) Impact response of cylindrically curved including a large deformation scaling study, International Journal of Impact Engineering,21(1-2)61-75

Krishnamurthy K.S, Mahajan P, Mittal R.K, (2001) A parametric study of the impact response and damage of

laminated cylindrical composite shells, Composites Science and Technology, 61(12) 1655-1669

Karmakar A., Kishimoto K. (2005) Transient Dynamic Response of Delaminated Composite Cylindrical Shells Subjected to Low-Velocity Impact, Key Engineering Material, 297-300 1285-1290

Karmakar A., Kishimoto K. (2006) Transient Dynamic Response of Delaminated Composite Rotating Shallow Shells Subjected to Low-Velocity Impact, Shock and Vibration13, 619-628.

Yiming F., Yiqi M., Yanping T. (2009) Damage analysis and dynamic response of elastoplastic laminated composite shallow spherical shell under the low-velocity impact, International Journal of Solids and Structures, 47 (1) 126–137

Sahoo S., Chakravorty, D., Finite element bending behavior of composite hyparbolic paraboloidal shells with various edge conditions, Journal of Strain Analysis for Engineering Design, 2004, 39 (5) 499-513

Sahoo S., Chakravorty, D. Finite element vibration characteristics of composite hypar shallow shells with various edge supports, Journal of Vibration and Control, 2005,11(10) 1291-1309.

Sahoo S., Chakravorty, D. Free vibration characteristics of point supported hypar shells – a finite approach, Advances in Vibration Engineering, 2008, 7(2) 197-205

Qatu, M. S., Leissa, A. W., 1991, 'Natural frequencies for cantilevered doubly-curved laminated composite shallow shells', Computers and Structures,17(3) 227-256

Das Neogi S., Karmakar A., Chakravorty, D., Impact Response of Simply Supported Skewed Hypar Shells Roofs by Finite Element, Journal of Reinforced Plastics and Composites, JRP-11-0246 (2011)

Received: 16th March 2023; Accepted: 03th August 2023; First distribution: 31th October 2023.